

Scaling of crack propagation in rubber sheets

This article has been downloaded from IOPscience. Please scroll down to see the full text article.

2011 EPL 96 36009

(<http://iopscience.iop.org/0295-5075/96/3/36009>)

View [the table of contents for this issue](#), or go to the [journal homepage](#) for more

Download details:

IP Address: 202.120.14.20

The article was downloaded on 20/04/2012 at 16:12

Please note that [terms and conditions apply](#).

Scaling of crack propagation in rubber sheets

C. H. CHEN¹, H. P. ZHANG¹, J. NIEMCZURA², K. RAVI-CHANDAR² and M. MARDER^{1(a)}

¹ Center for Nonlinear Dynamics and Department of Physics, The University of Texas at Austin
Austin, TX 78712, USA

² Center for Mechanics of Solids, Structures and Materials and Department of Aerospace Engineering
and Engineering Mechanics, The University of Texas at Austin - Austin, TX 78712, USA

received 8 July 2011; accepted in final form 12 September 2011

published online 24 October 2011

PACS 62.20.mt – Cracks

PACS 62.20.mm – Fracture

PACS 82.35.Lr – Physical properties of polymers

Abstract – We have conducted experiments and numerical simulations to investigate supersonic cracks. The experiments are performed at 85 °C to suppress strain-induced crystallites that complicate experiments at lower temperature. Calibration experiments were performed to obtain the parameters needed to compare with a theory including viscous dissipation. We find that both experiments and numerical simulations support supersonic cracks, and we discover a transition from subsonic to supersonic as we plot experimental crack speed curves *vs.* extension ratio for different sized samples. Both experiments and simulations show two different scaling regimes: the speed of subsonic cracks scales with the elastic energy density while the speed of supersonic cracks scales with the extension ratio. Crack openings have qualitatively different shapes in the two scaling regimes.

Copyright © EPLA, 2011

Introduction. – Our motivation in this letter is to investigate a fundamental question in fracture mechanics: “How fast can cracks propagate in brittle materials?”. It was long believed that a crack cannot propagate faster than sound speeds [1,2]. A single crack in a brittle material can accelerate by consuming elastic energy stored when material is stretched. But there seems to be a limiting speed for crack motion. Transport of stored energy to the crack tip is described by an energy flux tensor, and once the crack speed exceeds a critical value—the Rayleigh wave speed—the integrated energy flux becomes imaginary or negative. Thus one reaches the conventional conclusion that “the *limiting crack speed* in modes I and II is the Rayleigh wave speed and in mode III, the shear wave speed.” ([2], p. 73). In materials such as brittle plastics or brittle crystals, cracks do not even reach the Rayleigh wave speed. Instead, crack tips become unstable and sprout complicated three-dimensional branches when cracks pass a lower critical speed, on the order of half of Rayleigh wave speed [3–5].

However, cracks in rubber are different. Natural rubber can prevent the micro-branching instability spontaneously and allows cracks to propagate faster than the speed

of sound [6]. According to a supersonic rupture theory developed to explain the observations, velocities of supersonic cracks should be independent of system size if strain is held constant, in contrast to subsonic cracks whose velocity is independent of system size if energy density is held constant [7]. Nevertheless it has not been possible to compare theory and experiment in detail. At room temperature and large strains, natural rubber undergoes an increase in toughness of several orders of magnitude due to strain crystallization, greatly complicating the velocity response of cracks [8].

In this letter we carry out experiments at 85 °C where the strain crystallization is suppressed. We obtain a satisfactory quantitative description of the supersonic cracks, and show that both subsonic and supersonic propagation obey the predicted scaling laws.

Experimental methods. – The purpose of our studies is to understand the relation between crack speed and extension ratio in rubber sheets for opening mode cracks. The sheets are 0.15 mm thick with mass density ρ is 930 kg/m³. Extension ratio is defined as the ratio of the length of stretched specimens to the original length. In our experiments, natural rubber sheets are stretched uni-axially over a range of extension states: the extension

^(a)E-mail: marder@chaos.ph.utexas.edu

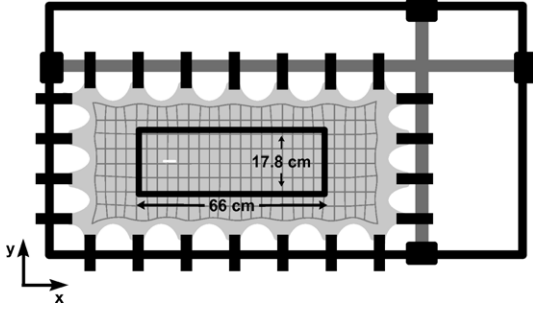


Fig. 1: Experimental setup for stretching rubber sheets in the vertical (y) direction. After the sheet has been extended to the desired state, it is clamped and a seed crack is initiated by cutting the sheet with a blade (white line, towards left of frame). A square grid is drawn on the sheet before it is stretched in order to measure the extension level as rubber is stretched.

ratio in the crack propagation (x) direction is constrained to be $\lambda_x = 1$, while the extension ratio λ_y along the loading (y) direction is varied between 1 and 5. The extension ratio in the thickness (z) direction is $\lambda_z = 1/(\lambda_x \lambda_y) = 1/\lambda_y$ because natural rubber is highly incompressible.

After rubber is stretched to a desired extension level, the sheet is clamped between a pair of rectangular steel frames. All frames have the same length 66 cm in the x -direction and different heights in the y -direction ($h = 5.1, 10.2,$ and 17.8 cm) as shown in fig. 1. A 1 mm long initial cut inserted into the prestretched sheet with a blade can result in either dynamic fracture propagation or a stationary fracture opening depending strongly on the stretched state [6,8,9]. Once the crack begins propagating, it reaches a steady state, typically within less than 0.1 s. The fracture resistance determines crack speeds and it is greatly enhanced by strains at room temperature. X-ray diffraction measurements of scattering intensity from the crystalline phase of rubber and systematic measurements of crack motion in rubber sheets, show that strain-induced crystallization occurs at 24°C when the extension ratio $\lambda_y > 3$. This toughening effect can be reduced by raising the temperature. We find that crack speeds increase monotonically with λ_y up to $\lambda_y = 5$ at 85°C [8]. All experiments mentioned in this letter were performed at 85°C for extension ratios $\lambda_y < 5$ so that crystallization should not be important.

We recorded crack motion with video at 48000 frames per second at a resolution of 384×256 pixels. By decorating the rubber sheet with ink marks and comparing consecutive frames we could extract particle velocities in the rubber sheet, as well as the velocity of the crack. Some results appear in fig. 5.

Numerical model. – We developed a computational model of rubber fracture with a minimal number of adjustable parameters and used it to compare with the experiments. At the continuum level, express deformations

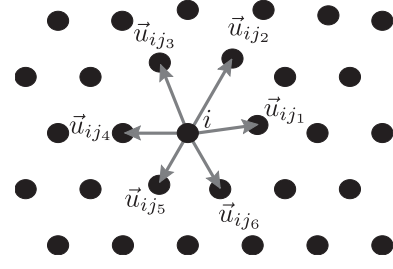


Fig. 2: Diagram showing triangular lattice of lattice spacing Δ .

in terms of finite strain tensor

$$E_{\alpha\beta} = \frac{1}{2} \left[\sum_{\gamma} \frac{\partial u_{\gamma}}{\partial r_{\alpha}} \frac{\partial u_{\gamma}}{\partial r_{\beta}} - \delta_{\alpha\beta} \right]. \quad (1)$$

Here $\vec{u}(\vec{r})$ describes the distance from the origin of a mass point that was located at \vec{r} when the rubber was relaxed.

We adopt an effective two-dimensional Mooney-Rivlin theory to describe the elastic behavior of thin rubber sheets [7]:

$$U/\rho = e_{\text{MR}} = a [I_1 + 2bI_2 + E_{zz}(1 + 2bI_1)], \quad (2)$$

where U has units of energy per volume, a is a constant with units of velocity squared, b is a dimensionless constant, $I_1 = E_{xx} + E_{yy}$, and $I_2 = E_{xx}E_{yy} - E_{xy}^2$, and

$$E_{zz} = \frac{1}{2} \left(\frac{1}{4I_2 + 2I_1 + 1} - 1 \right). \quad (3)$$

Our numerical approach is to consider microscopic interactions between mass points in a discrete lattice model that produce the rubber constitutive equation, eq. (2), in the continuum limit, but break when the separation between mass points is large enough. The lattice model is made up of a two-dimensional network of mass points which are connected with elastic bonds to six nearest neighbors to form a triangular lattice as shown in fig. 2. Take the original bond length between particles i and j to be Δ_{ij} . To obtain a numerical expression of the strain invariants, let $\vec{u}_{ij} \equiv \vec{u}_j - \vec{u}_i$, let $n(i)$ refer to the nearest neighbors of i , and define

$$F_i = \frac{1}{6} \sum_{j \in n(i)} \begin{cases} (\vec{u}_{ij} \cdot \vec{u}_{ij} / \Delta_{ij}^2 - 1), & \text{if } u_{ij} / \Delta_{ij} < \lambda_f, \\ \lambda_f^2 - 1, & \text{else,} \end{cases} \quad (4)$$

$$K_i = \begin{cases} \frac{1}{18} \sum_{j \neq k \in n(i)} \frac{(\vec{u}_{ij} \times \vec{u}_{ik})^2}{\Delta_{ij}^2 \Delta_{ik}^2}, & \text{for } K_i < K_{\text{max}}, \\ K_{\text{max}}, & \text{else.} \end{cases} \quad (5)$$

The quantity K_i has not previously been introduced in publications on this method [7]. From these numerical quantities, one can form representations of the strain invariants as follows:

$$I_1^i = F_i, \quad (6)$$

$$I_2^i = K_i/4 - F_i/2 - 1/4, \quad (7)$$

and finally construct the energy from

$$U = \sum_i m e_{\text{MR}}(I_1^i, I_2^i), \quad (8)$$

where m is the mass in a unit cell, and the energy density e_{MR} is given by eq. (2).

In the continuum limit,

$$\begin{aligned} K_i &= \frac{1}{18} \sum_{j \neq k \in n(i)} \frac{(\vec{u}_{ij} \times \vec{u}_{ik})^2}{\Delta_{ij}^2 \Delta_{ik}^2} \\ &= (2E_{xx} + 1)(2E_{yy} + 1) - (2E_{xy})^2 = 4I_2 + 2I_1 + 1. \end{aligned}$$

From eq. (3), $K_i = 1/(2E_{zz} + 1) \approx \lambda_z^{-2}$; K_i is approximately the inverse square of the extension ratio in thickness direction λ_z .

If the criterion for rupture is that λ_f is a constant, then cracks in numerical rubber undergo a tip-splitting instability well below the shear wave speed that prevents them from reaching supersonic speeds. To account for experimental observations in rubber, it is necessary to suppress these instabilities. This task was accomplished previously in an *ad hoc* way by making the bonds into a node tougher when two of the bonds attached to it had already broken [7]. Making use of the physical interpretation of K_i we posit a failure criterion that makes physical sense and leads to the desired type of toughening. The failure criterion is

$$\lambda_f = \lambda_f^0 + g/K \approx \lambda_f^0 + g\lambda_z^2. \quad (9)$$

Here λ_f^0 and g are constants. The failure criterion can be interpreted as saying that the sheet ruptures more easily when it has been stretched thin. The particular functional form $1/K_i$ is chosen for simplicity absent any direct evidence that another form should be preferred. The way this failure criterion stabilizes crack tips is that in the wake of the tip, the rubber contracts perpendicular to the direction of crack motion, and by contracting becomes thicker and therefore tougher. Numerical simulation bears out this physical reasoning, since simulations using eq. (9) in fact can produce supersonic cracks.

The complete equation of motion of particle i reads

$$m \frac{\partial^2 u_i^\alpha}{\partial t^2} = - \frac{\partial U}{\partial u_i^\alpha} - \beta \frac{\partial^2 U}{\partial t \partial u_i^\alpha}, \quad (10)$$

where the final term represents Kelvin dissipation with a dissipation parameter, β . The fact that nothing but dissipation is added to the equation of motion is a severe simplification. Rubber is hysteretic, and its strain-rate dependence is much more complicated than can be captured by a Kelvin model [10–12]. However, it appears that the very simple choice of dissipation allows adequate comparison with the collection of experiments described in this paper.

Determination of parameters. – The experimentally determined sound speeds (or elastic modulus) are used to calibrate the Mooney-Rivlin model [6]. Experimentally, the dimensionless parameter b in eq. (2) is 0.053 (at 24 °C), so in a first theoretical account one can set $b=0$. In this approximation the Mooney-Rivlin energy density e_{MR} reduces to the Neo-Hookean energy density

$$e_{\text{MR}} \approx e_{\text{NH}} = a(I_1 + E_{zz}). \quad (11)$$

This simple expression provides an adequate although not exceeding accurate description of rubber over the range of extensions in our experiments. The parameter a is directly related to sound speeds. We obtain it through fits to stress *vs.* extension in the range where the extension ratio λ_y ranges from 1 to 2. Reference [6] showed in experiments at 24 °C that this procedure is in good accord with time-of-flight measurements. We also measured stress-extension curves at 80 °C and found that sound speed increases slightly above the room temperature value [13]. In our simulations we use $a = 686.44 \text{ (m/s)}^2$ and $c_s = 26.2 \text{ m/s}$ at the temperature of 85 °C.

The simulations still depend upon three unknown parameters; β , λ_f^0 , and g . The dissipation parameter β was obtained from experiments in which bands of rubber were allowed to undergo free retraction. This was done by stretching a rubber band, releasing it, waiting for a retraction front to develop, and measuring its acceleration with video images [14]. These results were compared with direct numerical simulations using eq. (10). The parameter β was modified in simulations until the calculated peak acceleration of the simulation matched the peak acceleration of the experiment. Since no bonds break in a retraction simulation, the only tunable parameter is β .

The only parameter in simulations not directly obtained from experiments is the failure extension ratio λ_f consisting of two components: the cutoff constant λ_f^0 and the coefficient g in the toughening rule of eq. (9). By fitting experimental and numerical crack speeds, we obtained $\lambda_f^0 = 4.1$, and $g = 100$. Results are quite insensitive to the value of g so long as it is large enough to keep the crack tip stable.

Assembling all experimentally derived parameters, we perform our simulations with values of $a = 686.44 \text{ (m/s)}^2$, $b = 0$, $\beta = 9 \times 10^{-6} \text{ s}$, and rupture extension $\lambda_f = 4.1 + 100 \lambda_z^{-2}$. We tested three numerical systems with heights of 180, 360, and 630 rows to match the actual specimens with 5.1 cm, 10.2 cm, and 17.8 cm height, respectively. The system was at least five times as wide as it is tall in the unstretched state. The system ran for more than 15000 time units ($> 0.2 \text{ s}$) to ensure it has approached a steady state.

Results and discussion. – In this section, we compare the crack speeds from the simulations with those from the experiments. For a Mooney-Rivlin material, longitudinal wave speed depends strongly on extension

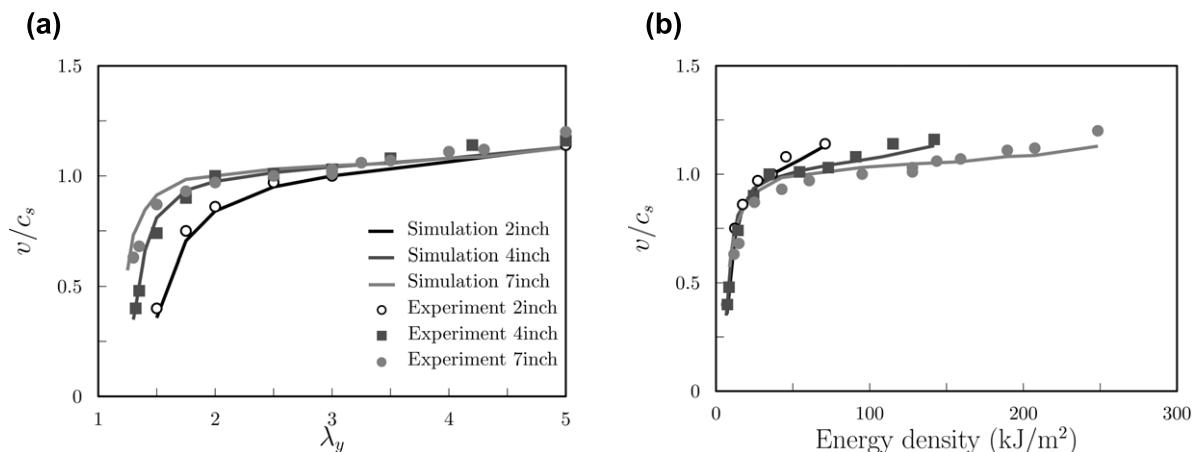


Fig. 3: Crack speed scaled by the shear wave speed as a function of the extension ratio λ_y in (a), and of the elastic energy density in (b). Both experimental results and simulations show two different scaling regimes for the crack speed. When we let Mooney-Rivlin constant b vary between 0 and 0.053, the numerical crack speeds only vary by 10%. All crack speeds are determined within the experimental error of ± 0.75 m/s.

but shear wave speed (c_s) behaves like a constant when extensions λ_x and λ_y on the order of 2 or greater [7]. Therefore, it makes sense to measure crack speeds in rubber in units of the shear wave speed. Our experimental and numerical crack speeds, scaled by the shear wave speed ($c_s = 26.2$ m/s at 85°C), are plotted as a function of extension ratio λ_y in fig. 3(a) and of the elastic energy density in fig. 3(b). Here, the elastic density is calculated as $E = e_{\text{NH}}(\lambda_y) h / \lambda_y$, where h is the height of the sample and e_{NH} is the Neo-Hookean elastic energy density as shown in eq. (11). Figure 3 shows that our numerical results based on the Neo-Hookean model are in agreement with the laboratory measurements. As we expect, both subsonic cracks ($v < c_s$) and supersonic cracks ($v > c_s$) are observed in three different sized samples. The transition from subsonic cracks to supersonic cracks occurs at about $\lambda_y = 2.0$ for the largest sample with 17.8 cm height, $\lambda_y = 2.5$ for samples with 10.2 cm height, and $\lambda_y = 3.0$ for samples of 5.1 cm height.

As predicted by supersonic rupture theory, there are two different scaling regimes for the crack speeds [7]. For subsonic cracks, crack speeds are independent of system size when plotted as a function of the elastic energy density E . This is the prediction of linear elastic fracture mechanics, worked out for example for cracks in strips by Marder [15] and verified in detail by Goldman *et al.* [16]. However, supersonic cracks in rubber sheets have quite different characteristics. Their crack speeds become independent of system size when plotted *vs.* λ_y rather than *vs.* elastic energy density shown in fig. 3. There is so much elastic energy stored in the vicinity of crack tip that it can support supersonic crack propagation and even provide extra energy to flow outwards. The crack speed is no longer limited by the time taken for the elastic energy from far away to flow into the crack tip [17].

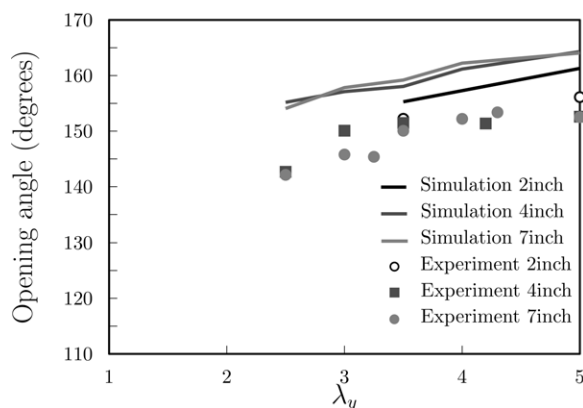


Fig. 4: Comparison of the rupture opening angles for supersonic cracks obtained from experimental results and numerical runs based on the Neo-Hookean energy model over a range of states where the extension ratio λ_y lies between 2.5 and 5. The simulations overestimate the angles around 10° systematically in all three sized samples. All crack speeds are determined within the experimental error of ± 0.75 m/s.

Furthermore, crack openings have a qualitatively different shape in two scaling regimes. Subsonic cracks have a parabolic tip as expected and the opening increases as λ_y increases; on the other hand, supersonic cracks have a wedge-like opening, with an opening angle of about 150° in experiment and 160° from numerics as shown in fig. 4. Figure 5 shows experimental and numerical measurements of velocity fields around a crack tip. The simulations slightly overestimate the openings and particle velocity, but otherwise theory and experiment correspond well.

Conclusion. – We measured properties of cracks in rubber at a temperature of 85°C and studied the

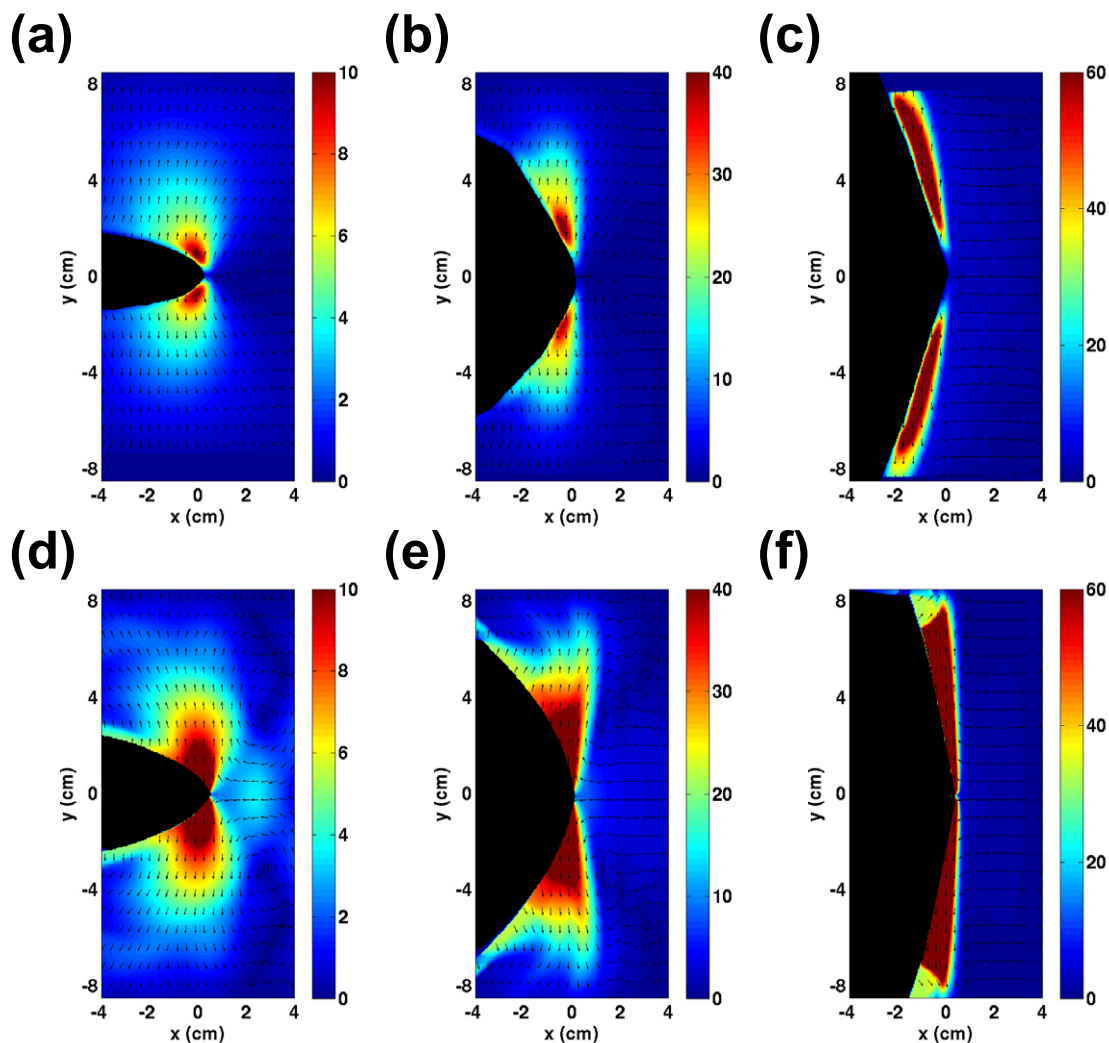


Fig. 5: (Color online) Top panels: images showing the experimental particle velocity fields of three steadily propagating cracks in $h = 17.8$ cm specimens: (a) $\lambda_y = 1.3$ and $v = 0.63 c_s$; (b) $\lambda_y = 1.75$ and $v = 0.93 c_s$; (c) $\lambda_y = 3.0$ and $v = 1.02 c_s$. The bottom panels show the particle velocity image of simulations compared to three experimental results which have the same crack speeds within 3% and extension ratios (d) $\lambda_y = 1.27$ and $v = 0.63 c_s$; (e) $\lambda_y = 1.6$ and $v = 0.95 c_s$; (f) $\lambda_y = 3.0$ and $v = 1.047 c_s$. Cracks propagate to the right, and black regions are the actual opening. The grayscale is coded according to the particle velocity and arrows show the direction of particle motion. We note that the particle velocity close to the crack tip is falsely represented in (c), because the velocity gradient in these regions is so large that the particle image velocimetry (PIV) algorithm cannot yield reliable results. The particle velocity fields in simulations are similar to those in experiments, but the opening angles of the ruptures are slightly larger than experimental results. Wedge-like openings are observed at $\lambda_y = 3.0$ in both experimental results (c) and simulations (f).

transition between subsonic and supersonic cracks. We also conducted numerical simulations based on a Neo-Hookean theory with Kelvin dissipation and a new rule for increasing toughness. This simple model produces satisfactory agreement with experiment for crack speeds and particle velocity fields. The experiments provide the first confirmation that supersonic cracks obey a scaling law in which speed naturally depends upon strain rather than energy density. The validity of this new scaling law implies that there exists a small characteristic scale length related to dissipative processes $\sim (\beta v)$ which is not present in linear elastic fracture mechanics, a scale-free

theory. Remaining quantitative inaccuracies, such as overestimation of opening angles and particle velocity, are likely related to the very simple equation of motion, eq. (10), employed for the simulations.

The authors acknowledge financial support from the United States National Science Foundation, Condensed Matter and Materials Theory program.

REFERENCES

- [1] FREUND L. B., *Dynamic Fracture Mechanics* (Cambridge University Press, Cambridge) 1990.
- [2] RAVI-CHANDAR K., *Dynamic Fracture* (Elsevier) 2004.
- [3] RAVI-CHANDAR K. and KNAUSS W. G., *Int. J. Fract.*, **26** (1984) 141.
- [4] FINEBERG J., GROSS S., MARDER M. and SWINNEY H., *Phys. Rev. Lett.*, **67** (1991) 457.
- [5] FINEBERG J. and MARDER M., *Phys. Rep.*, **313** (1999) 1.
- [6] PETERSAN P. J., DEEGAN R. D., MARDER M. and SWINNEY H. L., *Phys. Rev. Lett.*, **93** (2004) 015504.
- [7] MARDER M., *J. Mech. Phys. Solids*, **54** (2006) 491.
- [8] ZHANG H. P., NIEMCZURA J., DENNIS G., RAVI-CHANDAR K. and MARDER M., *Phys. Rev. Lett.*, **102** (2009) 245503.
- [9] LAKE G. J., LAWRENCE C. C. and THOMAS A. G., *Rubber Chem. Technol.*, **73** (2000) 801.
- [10] MOTT P. H. and ROLAND C. M., *J. Acoust. Soc. Am.*, **111** (2002) 1782.
- [11] NIEMCZURA J. G., *On the response of rubbers at high strain rates*, PhD Thesis, The University of Texas at Austin (2009).
- [12] NIEMCZURA J. and RAVI-CHANDAR K., *Contin. Mech. Thermodyn.*, **22** (2010) 469.
- [13] BOYCE M. and ARRUDA E., *Rubber Chem. Technol.*, **73** (2000) 504.
- [14] NIEMCZURA J. and RAVI-CHANDAR K., *J. Mech. Phys. Solids*, **59** (2011) 457.
- [15] MARDER M., *Phys. Rev. Lett.*, **66** (1991) 2484.
- [16] GOLDMAN T., LIVNE A. and FINEBERG J., *Phys. Rev. Lett.*, **104** (2010) 114301.
- [17] BOUCHBINDER E., FINEBERG J. and MARDER M., *Annu. Rev. Condens. Matter Phys.*, **1** (2010) 371.